

SRI International

October 13, 1988

MATHEMATICAL MODELING AND ECONOMIC ANALYSIS OF MEMBRANE SEPARATION OF HYDROGEN FROM GASIFIER SYNTHESIS GAS

Mathematical Modeling Topical Report

By: D. L. Roberts and D. E. Gottschlich

Prepared for:

MEMBRANE TECHNOLOGY AND RESEARCH, INC.
1360 Willow Road
Menlo Park, CA 94025

Attn: Richard W. Baker, President

Subcontract for U. S. Department of Energy
RFP-DE-RP-21-85MC22130

Approved:


Jerry L. Jones, Laboratory Director
Chemical Engineering Laboratory

G. R. Abrahamson
Senior Vice President
Sciences Group

DISTRIBUTION OF THIS DOCUMENT IS UNLIMITED

Deh

fr
7/28/92

MASTER



CONTENTS

SUMMARY	v
I. INTRODUCTION	1
II. THEORY	2
Cross Flow Configuration	3
Countercurrent Configuration	10
III. COMPARISON OF MODEL AND EXPERIMENTAL RESULTS	14
IV. MEMBRANE SYSTEM CONFIGURATIONS	21
Choice of Pressure Ratio	21
Single Module Configurations	23
Series Configuration	26
Cascade Configuration	28
Two Modules with Different Membranes	30
V. MEMBRANE SYSTEM EXAMPLES	33
Example Application	34
Performance Calculation Results.....	36
VI. CONCLUSIONS	46
REFERENCES	47

DISCLAIMER

This report was prepared as an account of work sponsored by an agency of the United States Government. Neither the United States Government nor any agency thereof, nor any of their employees, makes any warranty, express or implied, or assumes any legal liability or responsibility for the accuracy, completeness, or usefulness of any information, apparatus, product, or process disclosed, or represents that its use would not infringe privately owned rights. Reference herein to any specific commercial product, process, or service by trade name, trademark, manufacturer, or otherwise does not necessarily constitute or imply its endorsement, recommendation, or favoring by the United States Government or any agency thereof. The views and opinions of authors expressed herein do not necessarily state or reflect those of the United States Government or any agency thereof.

FIGURES

II-1	Cross Flow Membrane Module	4
II-2	Countercurrent Membrane Module	11
IV-1	Effect of Pressure Ratio on the Maximum Permeate Mole Fraction with Various Selectivities	22
IV-2	Effect of Pressure Ratio on the Maximum Permeate Mole Fraction with Various Feed Purities	24
IV-3	Single Module Configurations for Gas Separation	25
IV-4	Series Configuration (SER) for Gas Separation	27
IV-5	Two Stage Cascade Configurations for Gas Separations	29
IV-6	Separation Systems Which Benefit from Inversely Selective Membranes	32
V-1	Processing Cost as a Function of Product Purity	37
V-2	Partial Feed Bypass Scheme	40
V-3	Processing Costs With and Without PFB	42
V-4	Processing Costs for the Four Different Configurations with PFB	43

TABLES

II-1	Assumptions used in Models of Cross Flow and Countercurrent Membrane Modules	6
II-2	Cross Flow Model Input and Output Parameters	10
III-1	Pure Gas Membrane Properties	14
III-2	Experimental Results for Separation of a Gas Mixture with a Spiral-Wound Membrane Module	16
III-3	Experimental Results and Model Predictions for Separation of a Gas Mixture with a Spiral-Wound Membrane Module	17
III-4	Calculated Membrane Properties from Mixed Gas Experiments..	18
V-1	Feed Conditions and Membrane Properties for Example Application	35
V-2	Processing Costs for Six Different Membrane System Configurations	44

SUMMARY

Recent increases in the price of natural gas have promoted wide interest in finding alternative feedstocks for the manufacture of hydrogen. Coal appears to be one of the most attractive of these alternative feedstocks, considering its abundance and stable price in the United States. However, the manufacture of hydrogen from synthesis gas produced from coal is expensive because much larger capital investments are required than for the traditional plants based on steam-methane reforming. We are studying hydrogen purification by membrane technology as a means to make the coal-to-hydrogen route economically attractive.

To allow prediction of membrane performance and to facilitate comparisons between membrane and other technologies (cryogenic distillation, pressure swing adsorption), we developed a mathematical model to describe the permeation process inside a membrane module. The results of this model were compared with available experimental data (separation of $\text{CO}_2/\text{O}_2/\text{N}_2$ mixtures). The model was first used to calculate the gas permeabilities from one set of mixed-gas experiments; the resulting permeabilities were then used to predict the results of the other mixed-gas experiments. The agreement between these predictions and the experimental data was good. However, model predictions using gas permeabilities obtained in pure gas experiments did not agree with the mixed-gas experimental data. We believe this disagreement is due to plasticization of the membrane by contact with CO_2 . These results indicate that data obtained from experiments with mixed-gas feeds are necessary to adequately predict membrane performance when CO_2 is present.

The performance of different system configurations, including one and two stages of membrane modules, was examined. The different configurations examined were single module (SM), single module with recycle (SMR), series (SER), and two stage cascade with interstage compression (CAS). In general, SM is the most economical configuration for producing

low purity products, SER for medium purity products, and CAS for high purity products.

We also found that in some cases it is more economical to treat only a part of the feed stream with the membrane system and to make a higher purity gas than necessary in the final product. This high purity stream is then mixed with the untreated feed to produce a final product of the desired purity. If this approach is used, SER is the most economical configuration for low and medium purity products, and CAS is the most economical configuration for high purity products.

I INTRODUCTION

Recent increases in the price of natural gas have promoted wide interest in finding alternative feedstocks for the manufacture of hydrogen. Coal appears to be one of the most attractive of these alternative feedstocks, considering its abundance and stable price in the United States. However, the manufacture of hydrogen from synthesis gas produced from coal is expensive because much larger capital investments are required than for the traditional plants based on steam-methane reforming. Improvements are being sought at each step of the process (i.e., coal gasification, water/gas-shift reaction, and hydrogen separation) to make the coal-to-hydrogen route economically attractive. Membrane-based gas separation techniques offer a potential for reducing the overall costs of producing hydrogen from coal.

Traditional methods of gas purification (i.e., adsorption in amines, caustics, potassium carbonates, and other solvents) as well as the more recent processes (i.e., cryogenic separation and pressure-swing adsorption) are expensive because of high capital requirements and high energy use. Membrane gas purification may prove economically more attractive when used in a number of locations in a coal gasification process (e.g., before or after the CO-shift reactor). Recent improvements in membrane materials allow their consideration in such applications, particularly in combination with lower temperature shift catalysts.

To allow prediction of membrane module performance and to facilitate comparisons between membrane and other technologies (cryogenic distillation, pressure swing adsorption), we have developed a mathematical model to describe the permeation process inside a membrane module.

II THEORY

The mechanism for gas permeation across polymer membranes generally accepted today is the solution-diffusion model (Matson et al., 1983). This model includes three steps that describe the transport of a gas molecule across the membrane: (1) sorption of the molecule into the polymer, (2) diffusion of the molecule through the polymer, and (3) desorption of the molecule from the polymer into the permeate stream. Applying Henry's and Fick's laws, the flux is given by

$$N_i = \frac{Q_i(P_o x_i - P_I y_i)}{\delta} \quad i = 1, NC \quad (1)$$

and

$$Q_i = H_i D_i \quad (2)$$

where

D_i - diffusion coefficient of species i , cm^2/s

H_i - solubility of species i , $\frac{\text{cm}^3(\text{STP})}{\text{cm}^3\text{-cm Hg}}$

N_i - flux of species i , $\frac{\text{cm}^3(\text{STP})}{\text{cm}^2\text{-s}}$

NC - number of species

Q_i - permeability of species i , $\frac{\text{cm}^3(\text{STP})\text{-cm}}{\text{cm}^2\text{-s-cm Hg}}$

P_0 = total feed pressure, cm Hg

P_I = total permeate pressure, cm Hg

x_i = local feed-side mole fraction of species i

y_i = local permeate-side mole fraction of species i

δ = membrane thickness, cm

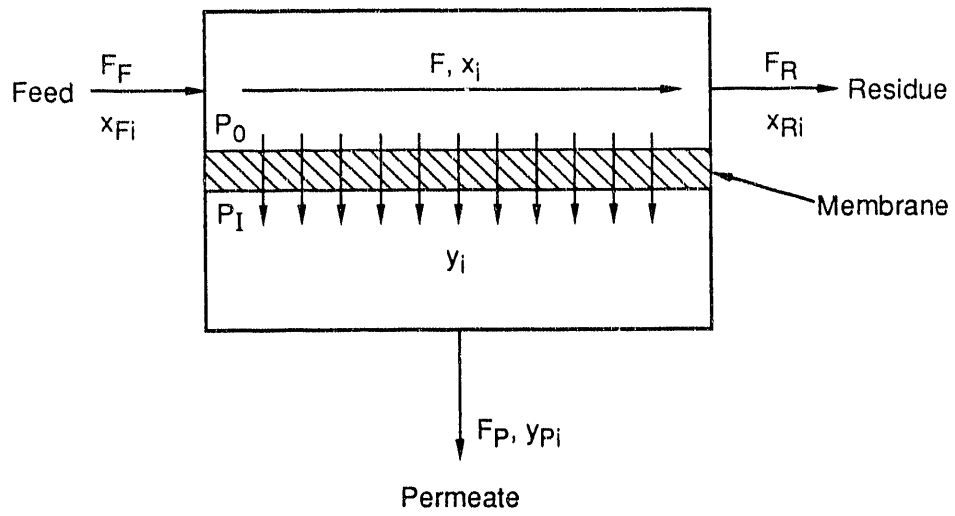
Often the values of H_i , D_i , and δ are not known precisely, and the ratio Q_i/δ is determined directly by experiment.

To model the membrane module, equation (1) will be used along with the assumption that Q_i is constant with respect to feed pressure and composition. Two models will be developed corresponding to two possible gas flow configurations: cross flow and countercurrent flow. The development of these models follows the procedure of Shindo et al. (1985).

Cross Flow Configuration

A cross flow module is illustrated in Figure II-1. If the local permeate composition is independent of the permeate composition at adjacent points on the membrane, as in a cross flow module, the local permeate composition, y_i , is given by

$$y_i = \frac{N_i}{\sum_{j=1}^{NC} N_j} \quad i = 1, NC \quad (3)$$



RA-M-360522-50A

Figure II-1. Cross-flow membrane module.

The local permeate mole fraction, y_i , is independent of the permeate composition at any other point in the module.

Upon substitution with equation 1, equation 3 becomes

$$y_i = \frac{Q_i(P_o x_i - P_I y_i)}{NC \sum_{j=1}^{NC} Q_j(P_o x_j - P_I y_j)} \quad i = 1, NC \quad (4)$$

To determine the y_i 's at any point along the membrane, the NC simultaneous equations represented by equation (4) must be solved. To solve these equations, we first divide y_1 (an arbitrarily chosen reference species) by the local permeate mole fraction of any other component:

$$\frac{y_1}{y_i} = \frac{Q_1(P_o x_1 - P_I y_1)}{Q_i(P_o x_i - P_I y_i)} \quad i = 2, NC \quad (5)$$

Upon rearrangement this equation becomes

$$y_i = \frac{x_i Q_i / Q_1}{P_I / P_o (Q_i / Q_1 - 1) + x_1 / y_1} \quad i = 2, NC \quad (6)$$

Using equation (6), we can determine all the y_i 's once y_1 is known. Since the sum of the mole fractions must equal 1.0, we have

$$\sum_{i=1}^{NC} \frac{x_i Q_i / Q_1}{P_I / P_o (Q_i / Q_1 - 1) + x_1 / y_1} - 1 = 0 \quad (7)$$

This equation depends only on y_1 and is easily solved using any one of a variety of root finding procedures. Once y_1 is known, the remaining y_i 's can be determined using equation (6), and equation (1) can be used to determine the individual component fluxes.

Equation (1) applies only at a single point on the membrane. To describe the performance of the entire module, we must account for changes in the feed-side composition (changes in x_i) along the length of the membrane. If F is the total feed-side volumetric flow rate and A is the membrane area, then the overall material balance across a differential area of membrane is given by

$$dF = - \sum_{i=1}^{NC} N_i dA \quad (8)$$

The change in feed-side flow rate along the length of the membrane is given by

$$\frac{dF}{dA} = - \sum_{i=1}^{NC} N_i \quad (9)$$

Equations (8) and (9) assume that the gas velocity distribution is flat (plug flow) and at steady state and that diffusion occurs only across the membrane (not along it). The assumptions used in the model are summarized in Table II-1.

Table II-1

ASSUMPTIONS USED IN CROSS FLOW AND
COUNTERCURRENT MEMBRANE MODULE MODELS

1. Transport of all species is by Fickian diffusion with constant diffusion coefficients.
2. Permeabilities are independent of pressure and composition.
3. Diffusion inside the membrane along the length of the membrane is negligible.
4. There is no gas phase mass transfer resistance.
5. The gas is in plug flow on both sides of the membrane.
6. The system is at steady state.
7. Pressure drops in feed, and permeate streams are negligible.

The individual component material balances are given by

$$d(Fx_i) = -N_i dA \quad i = 1, NC \quad (10)$$

Therefore, the change in feed-side mole fraction along the membrane is given by

$$\frac{dx_i}{dA} = \frac{-N_i}{F} + \frac{x_i}{F} \frac{dF}{dA} \quad i = 1, NC \quad (11)$$

Since the membrane area is usually not independent, but is determined by the operating conditions, we will change the independent variable from the membrane area to the mole fraction of component 1 in the residue stream. Equations (9) and (11) become

$$\frac{dF}{dx_1} = \left(\frac{dF}{dA} \right) \left(\frac{dx_1}{dA} \right)^{-1} \quad (12)$$

and

$$\frac{dx_i}{dx_1} = \left(\frac{dx_i}{dA} \right) \left(\frac{dx_1}{dA} \right)^{-1} \quad i = 2, NC \quad (13)$$

The boundary conditions are

At the feed inlet ($x_A = x_{FA}$),

$$A = 0$$

$$F = F_F$$

$$x_i = x_{Fi} \quad i = 1, NC$$

The equations are nondimensionalized using the following transformations:

$$N_i^* = \frac{N_i}{Q_1 P_o / \delta} \quad (14)$$

$$A^* = \frac{Q_1 P_o}{\delta F_F} A \quad (15)$$

$$F^* = \frac{F}{F_F} \quad (16)$$

$$\gamma = \frac{P_I}{P_o} \quad (17)$$

$$\alpha_i = Q_i / Q_1 \quad (18)$$

The differential equations 12 and 13 become the nondimensional equations

$$\frac{dA^*}{dx_1} = \left[\frac{-N_1^*}{F^*} + \frac{x_1}{F^*} \left(\frac{dF^*}{dA^*} \right) \right]^{-1} \quad (19)$$

$$\frac{dF^*}{dx_1} = \left(\frac{dA^*}{dx_1} \right) \sum_{i=1}^{NC} N_i^* \quad (20)$$

$$\frac{dx_i}{dx_1} = \left(\frac{dA^*}{dx_1} \right) \left[\frac{-N_i^*}{F^*} + \frac{x_i}{F^*} \left(\frac{dF^*}{dA^*} \right) \right] \quad i = 2, NC \quad (21)$$

and the boundary conditions become

At the feed inlet ($x_A = x_{FA}$),

$$\begin{aligned} A^* &= 0 \\ F^* &= 1.0 \\ x_i &= x_{Fi} \quad i = 1, NC \end{aligned}$$

Equations (19), (20), and (21) are integrated from $x_1 = x_{F1}$ to $x_1 = x_{R1}$, and the results are the residue stream flow rate and composition, and the membrane area. The permeate stream flow rate and composition are found by material balances:

$$F_P^* = 1 - F_R^* \quad (22)$$

$$y_{Pi} = \frac{x_{Fi} - F_R^* x_{Ri}}{1 - F_R^*} \quad i = 1, NC \quad (23)$$

F_P^* and F_R^* are the dimensionless permeate and residue stream flow rates. The fractional recovery of component 1 in the permeate stream is given by

$$\theta = \frac{x_{F1}}{y_{P1}(1 - F_R^*)} \quad (24)$$

The integration is carried out numerically using the Runge-Kutta procedure written by Sandia Laboratories (Shampine et al, 1975). A summary of the input and output information is given in Table II-2.

Although this set of input and output parameters is very useful, there are times when, for example, x_{R1} is not known but y_{P1} is known. To make the model more general in this respect, the computer program contains a procedure that allows one of the output parameters listed in Table II-2 to be specified as an input parameter and one of the first

Table II-2

CROSS FLOW MODEL INPUT AND OUTPUT PARAMETERS

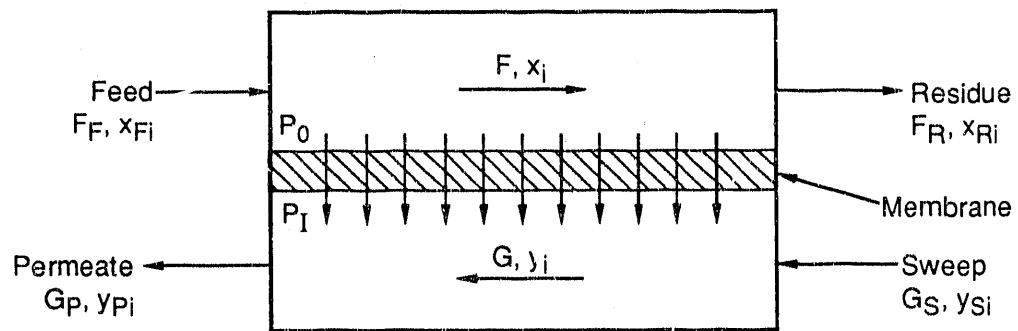
Input	Output
1. x_{F1}, \dots, x_{FNC}	1. F_R
2. γ	2. x_{R2}, \dots, x_{RNC}
3. Q_1, \dots, Q_{NC}	3. y_{P1}, \dots, y_{PNC}
4. x_{R1}	4. θ
5. F_F	
6. P_o	
7. δ	
8. T	

four input parameters to be calculated by the program. Calculations made with this alternative list of input and output parameters drastically increases the computer time and is avoided whenever possible.

Countercurrent Configuration

A countercurrent flow configuration is used in many separation processes (such as stripping, absorption, distillation) because this configuration results in the greatest average driving force for separation. The same advantage applies to membrane separators that operate with countercurrent flow (Figure II-2). The permeate composition at a point in a countercurrent module depends on both the ratio of fluxes across the membrane and the permeate composition immediately upstream of that point.

The development of the countercurrent model is similar to that of the cross flow model, except the local permeate composition, y_i , is determined by material balance instead of by flux ratios as in equation (6). However, at the sweep inlet, where the permeate side flow



RA-M-1732-14

Figure II-2. Countercurrent membrane module.
 The permeate composition, y_i , is dependent upon the permeate composition directly upstream of that point.

rate is zero, the permeate composition is determined by flux ratios. In the countercurrent model, the dimensionless area, A^* , is the independent variable. The assumptions are the same as used for the cross flow model (see Table II-1). The equations describing a countercurrent module are

$$N_i^* = \alpha_i (x_i - \gamma y_i) \quad (25)$$

$$\frac{dF^*}{dA^*} = - \sum_{i=1}^{NC} N_i^* \quad (26)$$

$$\frac{dx_i}{dA^*} = \frac{-N_i^*}{F} + \frac{x_i}{F} \sum_{j=1}^{NC} N_j^* \quad (27)$$

$$y_i = \frac{G_s^* y_{si} + x_i F^* - F_R^* x_{Ri}}{G_s^* + F^* - F_R^*} \quad (28)$$

In these equations, G is the permeate-side flow rate. Equations (14) through (18) still apply, and we define

$$G^* = \frac{G}{G_F}$$

The boundary conditions are

At the feed end ($A^* = 0$)

$$x_i = x_{Fi}$$

$$F^* = 1$$

At the residue end ($A^* = A_T^*$)

$$y_i = y_{si}$$

$$G^* = G_s^*$$

Equations (26) and (27) are solved by numerically integrating from one end of the membrane to the other. Because the conditions of only one of the two streams at each end of the module are known, the integration can be started at either end. In our model, integration begins at the residue/sweep end and proceeds towards the feed/permeate end. Thus, integration is from $A = A_T$ to $A = 0$. Since the flow rate and composition of the residue stream are not known, their values must initially be guessed before the integration can be started. The integration is performed by the Runge-Kutta procedure also used in the cross flow model. When integration reaches $A = 0$, the calculated values for the feed flow rate and composition can be compared with the actual values. If they are within a given tolerance, the calculated solution is valid. Otherwise, new guesses for the residue flow rate and composition are made, and the process is repeated until the correct solution is found.

Further development of this model (such as changing the independent variable to x_{R1}) was discontinued at this point for two reasons. First, the spiral-wound modules under development by Membrane Technology and Research (MTR) are not operated in a countercurrent gas flow configuration. Second, Pan (1986) shows that for asymmetric membranes, including most present-day gas separation membranes (such as MTR's membranes), the cross flow model best describes the module performance even when the module uses a countercurrent flow scheme.

III COMPARISON OF MODEL AND EXPERIMENTAL RESULTS

To test the accuracy of the model predictions, we compared the predictions with experimental results obtained using a spiral-wound module. The module performance tests using a mixed-gas feed for this project had only just begun at the time of writing of this report, so the experimental results used for evaluating the model were obtained from a previous MTR project. The experimental module was manufactured by MTR and contained 2000 cm² of a silicone rubber membrane. The feed mixture used in this test consisted of CO₂, O₂, and N₂. The pressure normalized fluxes, PNF (permeability/membrane thickness), obtained using pure gases in the module are given in Table III-1.

Table III-1

PURE GAS MEMBRANE PROPERTIES

<u>Gas</u>	PNF $\left(\frac{\text{cm}^3(\text{STP})}{\text{cm}^2\text{-s-cmHg}} \right)$
CO ₂	2.3 x 10 ⁻³
O ₂	0.48 x 10 ⁻³
N ₂	0.25 x 10 ⁻³

The experiments were performed using two different feed mixtures (case I - 0.3% CO₂, 18.9% O₂, 80.8% N₂; case II - 10.4% CO₂, 16.6% O₂, 73.0% N₂), each at several feed flow rates. The results (residue and permeate compositions and feed fraction permeated [FFP]) are included in Table III-2. Because of experimental error the residue and permeate compositions obtained during the experiments are somewhat inconsistent (i.e., a material balance around the module does not close). Since the

model rigorously conserves mass, the model can never exactly agree with these experimental results. As a measure of the deviation from conservation of mass we have defined the following parameter:

$$E_r = \sum_{i=1}^{NC} \text{abs} \left[1 - \frac{x_{Fi}}{(1-FFP)x_{Ri} + (FFP)y_{Pi}} \right] \quad (29)$$

The value of E_r for each experiment is included in Table III-2.

The model predictions were obtained by specifying that the predicted FFP is equal to the reported value, and the pressure ratio used by the model is the experimentally reported value. The model then predicts the residue and permeate compositions and the required membrane area. Two sets of model predictions were produced. The first used the pure gas PNFs to predict the results. These predictions are listed in Table III-3 on the lines beginning "Model (pure gas PNFs)." The second set of predictions was obtained by varying the PNFs to cause the predictions to fall within 2.5% of the experimental values. For each of the two cases, the experiment which had the lowest E_r was used for calculating the PNF values (experiment I.2 for case I and II.1 for case II). These calculated values of the pressure normalized flux were then used to predict the experimental results obtained at the other feed flow rates. This set of predictions is included in Table III-3 on the lines beginning with "Model (calculated PNFs)." The calculated values of PNF obtained for each feed mixture are included in Table III-4. In all cases using pure gas PNFs, the model predicts better separation than is actually obtained in the experiment; the predicted CO_2 fraction in the residue is less than the experimental value, the predicted CO_2 fraction in the permeate is greater than the experimental result, and the predicted membrane area is less than the actual area of the module.

Table III-2

EXPERIMENTAL RESULTS FOR SEPARATION OF A GAS MIXTURE
WITH A SPIRAL-WOUND MEMBRANE MODULE

Case	Experiment Number	Feed Flow (λ (STP)/min)	Feed Fraction Permeated(FFP)	Residue Composition(%)		Permeate Composition (%)			E_r	
				CO ₂	O ₂	N ₂	CO ₂	O ₂		N ₂
I	I.1	11.2	0.197	0.17	16.7	83.1	0.90	29.2	69.9	0.061
I	I.2	7.2	0.304	0.11	15.0	84.9	0.74	28.5	70.8	0.018
I	I.3	3.4	0.639	0.02	9.6	90.4	0.46	24.7	74.9	0.026
II	II.1	13.0	0.211	6.3	15.8	77.9	24.6	20.4	55.0	0.035
II	II.2	8.3	0.333	4.2	14.9	80.9	21.9	20.5	57.6	0.042
II	II.3	5.3	0.523	1.8	13.1	85.1	17.6	20.4	62.0	0.053

Table III-3

EXPERIMENTAL RESULTS AND MODEL PREDICTIONS
FOR SEPARATION OF A GAS MIXTURE
WITH A SPIRAL-WOUND MEMBRANE MODULE

Experiment	Feed Flow (λ (STP)/min)	Feed Fraction Permeated(FFP)	Residue Composition(%)			Permeate Composition (%)			Membrane Area (cm^2)
			CO ₂	O ₂	N ₂	CO ₂	O ₂	N ₂	
I.1	Experiment data	0.197	0.17	16.7	83.1	0.90	29.2	69.9	2000
	Model (pure gas PNFs) *	0.197	0.094	16.6	83.3	1.14	28.4	70.4	1710
	Model (calculated PNFs †)	0.197	0.163	16.4	83.5	0.86	29.2	70.0	1990
I.2	Experiment data	0.304	0.11	15.0	84.9	0.74	28.5	70.8	2000
	Model (pure gas PNFs) *	0.304	0.043	15.1	84.8	0.89	27.6	71.6	1720
	Model (calculated PNFs †)	0.304	0.109	14.9	85.0	0.74	28.2	71.1	2000
I.3	Experiment data	0.639	0.02	9.6	90.4	0.46	24.7	74.9	2000
	Model (pure gas PNFs) *	0.639	0.001	9.64	90.4	0.47	24.1	75.4	1760
	Model (calculated PNFs †)	0.639	0.016	9.14	90.8	0.46	24.4	75.1	2050
II.1	Experiment data	0.211	6.3	15.8	77.9	24.6	20.4	55.0	2000
	Model (pure gas PNFs) *	0.211	4.36	15.9	79.7	33.0	19.1	47.9	1550
	Model (calculated PNFs †)	0.211	6.45	15.7	77.9	25.2	20.0	54.8	2000
II.2	Experiment data	0.333	4.2	14.9	80.9	21.9	20.5	57.6	2000
	Model (pure gas PNFs) *	0.333	2.08	14.9	83.1	27.1	20.1	52.9	1670
	Model (calculated PNFs †)	0.333	4.44	14.8	80.7	22.4	20.2	57.5	2060
II.3	Experiment data	0.523	1.8	13.1	85.1	17.6	20.4	62.0	2000
	Model (pure gas PNFs) *	0.523	0.40	12.3	87.3	19.5	20.6	59.9	1840
	Model (calculated PNFs †)	0.523	1.97	12.9	85.2	18.1	20.0	61.9	2160

* Calculated PNF values for case I were obtained using results from experiment I.2.

† Calculated PNF values for case II were obtained using results from experiment II.1.

Table III-4

CALCULATED MEMBRANE PROPERTIES FROM
MIXED GAS EXPERIMENTS

Gas	PNF $\left(\frac{\text{cm}^3(\text{STP})}{\text{cm}^2 \cdot \text{S} \cdot \text{cmHg}} \right)$	
	Case I	Case II
CO ₂	1.06 x 10 ⁻³	1.05 x 10 ⁻³
O ₂	0.43 x 10 ⁻³	0.40 x 10 ⁻³
N ₂	0.21 x 10 ⁻³	0.23 x 10 ⁻³

For each case, when the fitted values of the pressure normalized flux are used to predict the results of the two experiments from which the PNFs were not calculated, the model predictions fall within 5% of the experimental results. (In two experiments, I.3 and II.3, the error in the CO₂ residue composition was greater than 5%. However, this large error may be due to the low number of significant figures in the reported data.) The fact that these predictions agree not only with the experimental results from which the PNFs were calculated, but also with the results at the other feed flow rates implies that the model does describe the process of mass transport across a membrane and the calculated PNFs are true physical properties, not simply a set of arbitrary values that allow us to match an individual set of experimental results. The calculated PNFs for the two different feed cases are very similar (the values are all within 8% of each other); this similarity in the calculated PNFs indicates that one set of experimental data can be used to predict module performance over a significant range of operating conditions.

Why there is such a large discrepancy between the pure gas and fitted values for PNF (the fitted PNF of CO₂ is less than 50% of the pure gas values, and the fitted PNFs of O₂ and N₂ are 80% to 90% of their pure

gas values) can be blamed in part on plasticization of the membrane by CO_2 (Chern et al, 1983). When CO_2 is absorbed by a polymer, the polymer becomes plasticized; that is, its structure becomes looser, and dissolved species can diffuse through the polymer more easily than when the polymer is not plasticized. As the CO_2 concentration in the polymer increases, the degree of plasticization also increases. Because the pure gas PNF of CO_2 was measured at a feed pressure of 1 atm (using the same module as in the mixture tests), the resulting value was obtained when the membrane was plasticized by a CO_2 partial pressure of 1 atm. However, in the mixture tests the membrane was plasticized by a CO_2 partial pressure of only 0.003 atm and 0.104 atm for cases I and II, respectively, and thus was less plasticized than when the pure gas PNF of CO_2 was measured. Therefore, the PNF of CO_2 with the mixed feed should be less than with the pure feed; this result was observed in the experiments.

When the pure gas PNFs of O_2 and N_2 were measured, no CO_2 was present, and therefore the membrane was not plasticized. With the mixed feed, however, the membrane was plasticized to some extent, and we would expect the pure gas PNFs of O_2 and N_2 to be less than the PNFs resulting from the mixture tests. However, the opposite was observed: the pure gas PNFs are greater than the mixture PNFs. Thus, plasticization by CO_2 cannot completely explain the discrepancy between the pure gas and calculated PNFs. Either there are other mixture interactions, or some experimental error also significantly affected the results from the module tests. Further experiments using a pure CO_2 feed at different pressures would be necessary to quantify the effect of plasticization on the PNFs.

MTR's results for the current project using poly-[ether-ester-amide] (PEEA) membranes (not modules) show a CO_2 PNF increase of approximately 50% between 100 psig and 300 psig (in pure gas experiments). Tests with CO_2/H_2 mixtures resulted in a reduction in selectivity from 8 (pure gas experiments) to 7 (mixed-gas experiments), implying that plasticization affects H_2 permeability to a greater extent than it does CO_2 permeability. Because plasticization causes only a small change in

selectivity for the PEEA membrane, the effort required to include plasticization in the model probably is not warranted. When mixture tests are performed for the present project, the model can be used to determine the mixture PNFs, and these PNFs can then be used in the model to more accurately predict the module performance at other conditions.

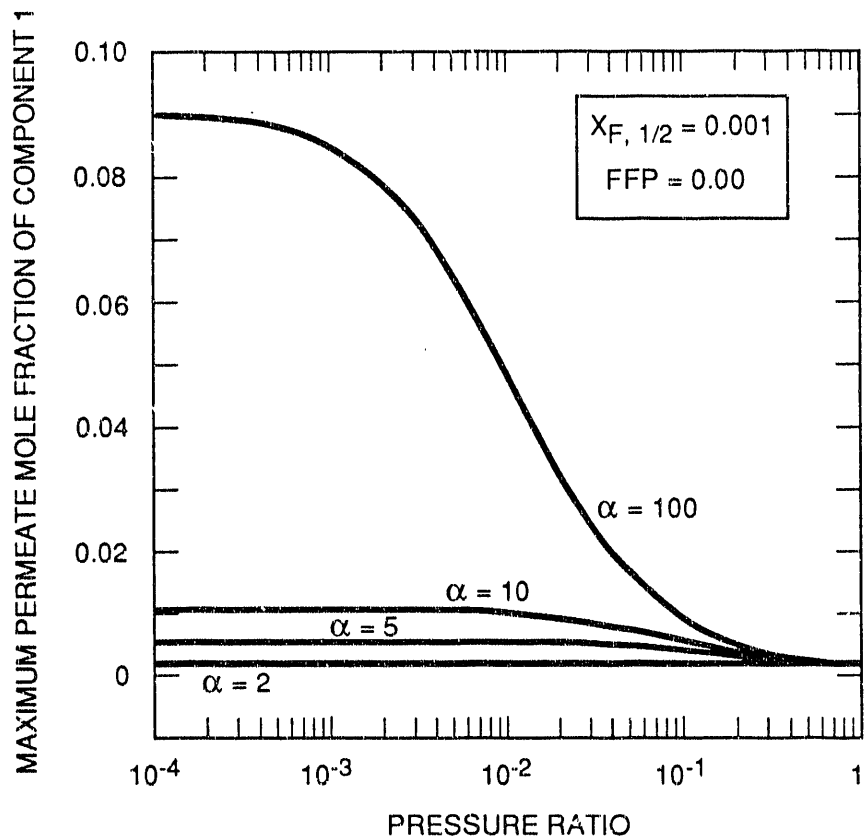
IV MEMBRANE SYSTEM CONFIGURATIONS

Once the model for an individual membrane module is completed, it can be used as a building block to describe the performance of an arrangement of several modules. A large number of possible arrangements could be used, including recycle streams, multiple stages, and variations in compressor positions. Because current commercial membrane systems with few exceptions are limited to one stage, this study will include configurations of no more than two cross flow modules.

Choice of Pressure Ratio

The pressure ratio across the membrane is normally a process variable whose value is at the discretion of the process designer. Practical constraints may intervene, however, such as when the feed pressure is fixed by an upstream process, or when the permeate pressure must be above atmospheric to avoid the use of vacuum pumps.

The various constraints and guidelines for estimating the optimum pressure ratio have been presented in prior papers (Pan and Habgood, 1974; Peinemann et al, 1986); however, it is useful to present them again here. In membrane systems, a larger pressure ratio causes a poorer degree of separation for a given membrane. Thus, there is a value of the pressure ratio beyond which a desired purity cannot be obtained. This constraint is illustrated in Figure IV-1, where the maximum permeate mole fraction decreases toward the feed composition as the pressure ratio is increased toward 1.0. In this figure, the calculations are made for a feed rate so large that the feed-side concentration does not change and the fraction of feed permeated approaches zero. This configuration results in the maximum permeate mole fraction (for component 1) from this system.



RA-M-1732-15

Figure IV - 1. Effect of pressure ratio on the maximum permeate mole fraction with various selectivities.

The pressure ratio limits the maximum permeate mole fraction when the pressure ratio is greater than approximately $\alpha^{-1.5}$.

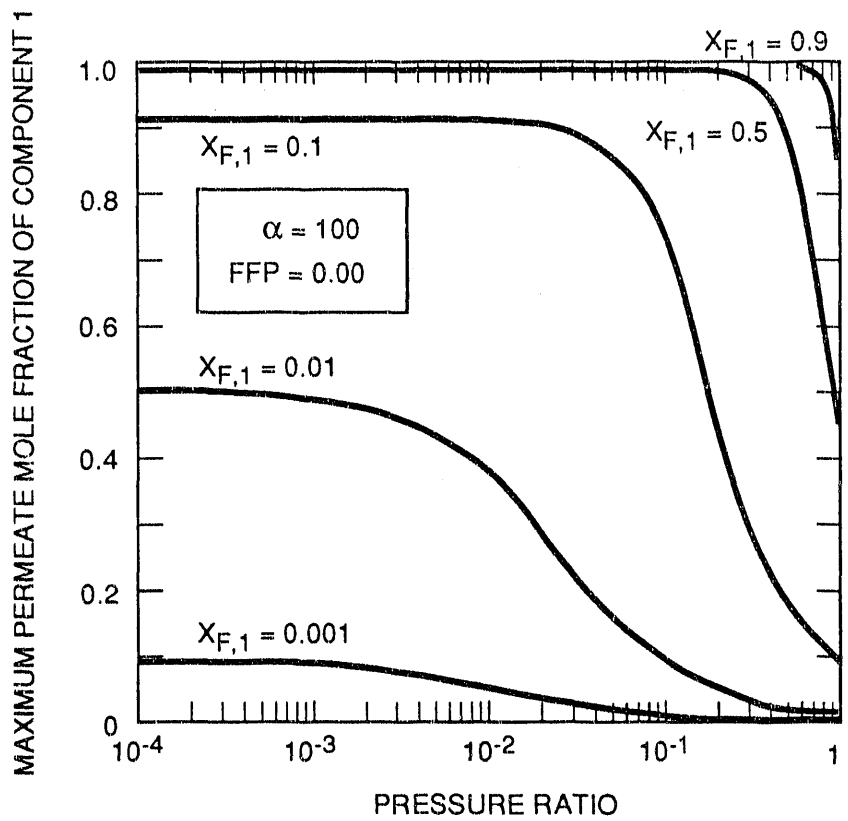
Figure IV-1 also illustrates the fact that as the pressure ratio is reduced, a point is reached at which any further reduction has no significant effect on membrane performance. As well, the point below which further reductions in pressure ratio have no effect is different for membranes of different selectivity; as the selectivity increases, this point takes on a smaller value. Thus, below a certain pressure ratio, the selectivity limits the degree of separation, while at higher pressure ratios, the pressure ratio limits the degree of separation.

The feed composition is also a controlling factor in membrane performance, and like selectivity, can affect the point at which further reductions in the pressure ratio have no effect on membrane performance. This effect is illustrated in Figure IV-2, which is similar to the previous figure except that instead of showing curves with different selectivities, it shows curves of different feed compositions. As the feed becomes more pure, the point below which pressure ratio has no effect gets closer to 1.0. Thus, for feeds of high purity nothing can be gained by using a small pressure ratio. Figures IV-1 and IV-2 show that, as a general rule, little can be gained by using a pressure ratio with a value more than one magnitude smaller than either (1) the feed mole fraction of the most permeable component or (2) the inverse of the selectivity.

The membrane area required to perform a given separation is less when a smaller pressure ratio is used (up to a point, as discussed above), but the compression expenses are greater. By assigning a cost to membrane area and to compression requirements (capital and operating), an optimum pressure ratio can be determined resulting in the lowest total cost for a given separation.

Single Module Configurations

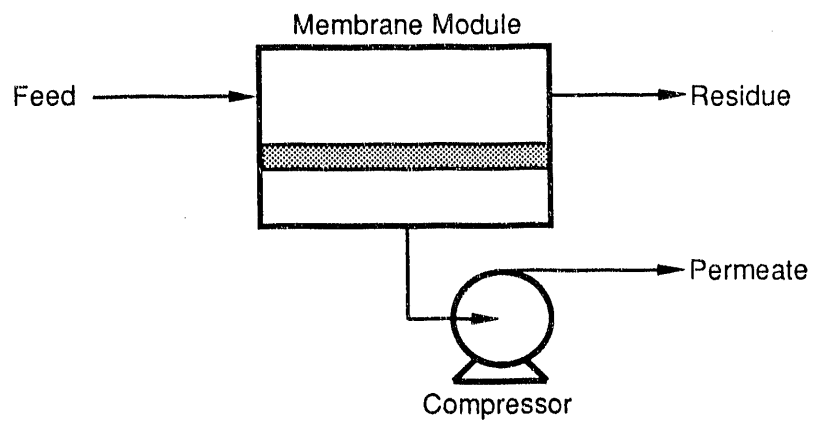
The basic single module configuration (SM) is shown in Figure IV-3. This basic gas separation configuration is described by the cross flow model previously developed. When the permeate purity requirement is fixed, reducing the pressure ratio increases the fraction of the most



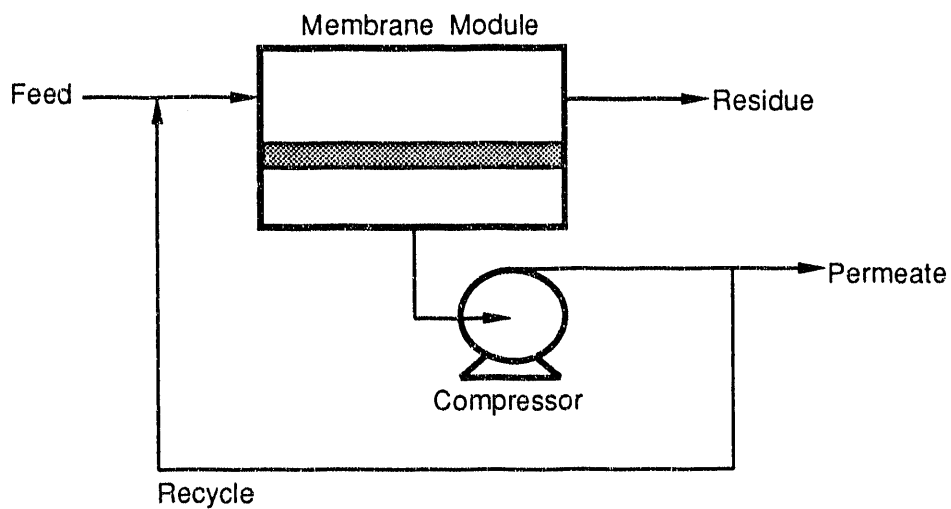
RA-M-1732-16

Figure IV - 2 Effect of pressure ratio on the maximum permeate mole fraction with various feed purities.

Reduction of pressure ratio to below the value of the feed mole fraction of component 1 has little effect on the maximum permeate mole fraction.



(a) Single module (SM)



(b) Single module with recycle (SMR)

RA-M-1732-17

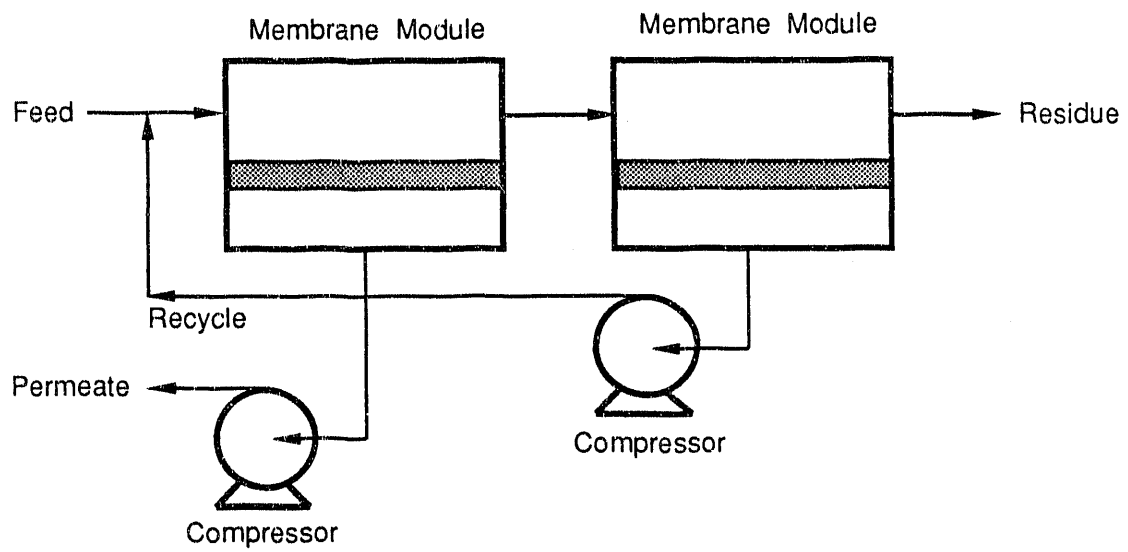
Figure IV-3. Single module configurations for gas separation.

permeable component, which is recovered in the permeate stream. Reducing the pressure ratio also increases the permeate purity that can be obtained with the membrane.

If part of the permeate stream is recycled back to the feed, the membrane feed will be more concentrated, and a more concentrated permeate can be obtained than is possible without recycle. The single module with recycle configuration (SMR) is shown in Figure IV-3. A drawback of the recycle configuration, however, is that the total flow through the module is increased by the recycle stream, which results in an increase in both the membrane area and compressor size. Both of these configurations, and the remaining configurations to be discussed, assume that the feed is available at pressure and that the product streams must also be at the feed pressure.

Series Configuration

To increase the degree of separation obtainable by the membrane system, we can add a second module, using as its feed either the first stage residue or permeate. When the residue from the first module is used as the feed to the second module, we term the configuration a series (SER) (Figure IV-4). In a membrane module, the most concentrated permeate is produced by the initial part of the membrane, where the feed-side concentration is the highest. Thus, in this configuration the permeate from the first module is the most concentrated and is the product stream. Because the residue from the second module may still contain a significant fraction of the component to be recovered, a second module is used to recover the remaining product, although at purities too low for use as product. This stream is therefore recycled back to the first module. To increase the fractional recovery of a component using this configuration, the recycle stream flow rate is increased. Reducing the permeate stream flow rate or increasing the recycle stream flow rate will improve the degree of separation, but it will also increase the per unit product cost.



RA-M-1732-18

Figure IV-4. Series configuration (SER) for gas separation.

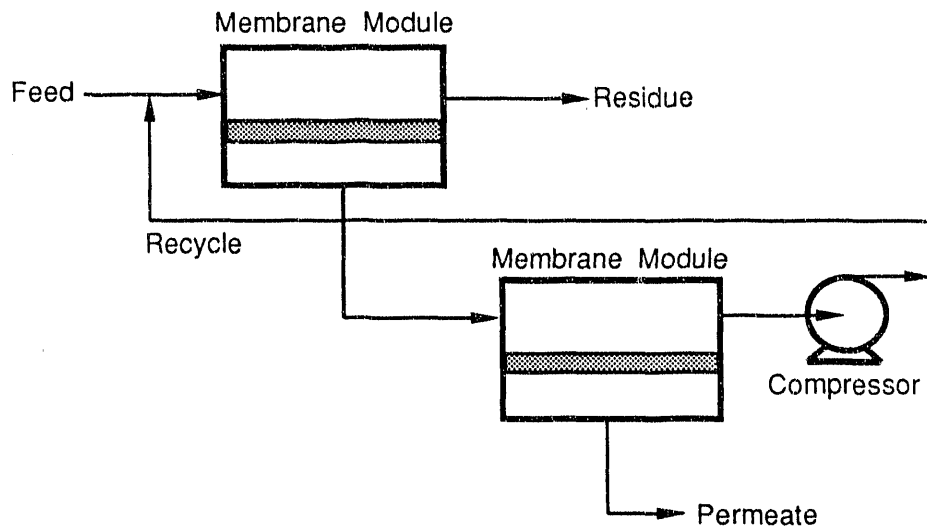
At this point it is useful to make a distinction between the terms "module" and "stage." A single membrane module has only one inlet stream (feed) and two outlet streams leaving the module (permeate and residue), as in configuration SM. A multi-module system may contain a number of modules and more than two outlet streams (multiple permeate, residue, and recycle streams) as in configuration SER. The number of stages is defined as the number of membranes separating the feed and overall permeate streams. (Configuration SER is a single-stage configuration, while the next configuration to be discussed, CAS, is a two-stage configuration.) A stage may contain any number of membrane modules.

Cascade Configuration

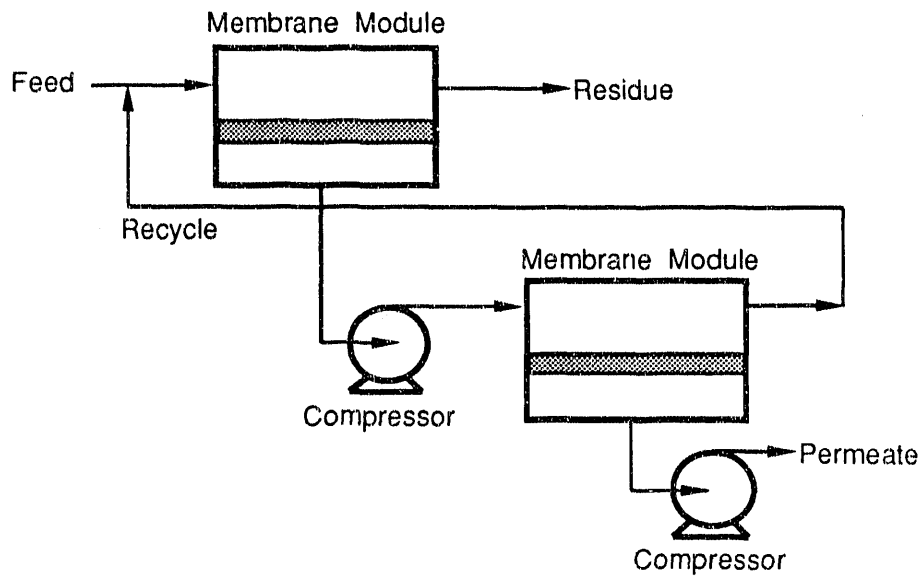
In the cascade configuration, shown in Figure IV-5, the first module permeate is used as the feed to the second module. In this way the concentrated stream from the first module is reconcentrated in the second module, and a more concentrated product can be obtained than with any of the previously described configurations. Because the feed and permeate are separated by two membranes, each module is a stage and the configuration is a two-stage configuration.

There are several possible locations for the compressors, the best location depending on several factors: the pressure at which the feed is available; whether or not the second stage residue is to be recycled; and the pressures at which the permeate and residue streams must be delivered. In Figure IV-5, two compressor arrangements are shown; in both cases, the feed is available at high pressure. In the recycle compression arrangement (CASR), the permeate delivery pressure is atmospheric, while in the interstage compression arrangement (CAS) the permeate is delivered at the feed pressure. In CASR, where only the recycle stream is compressed, the capital and operating costs are lower than for CAS which requires compression of a larger volume of gas.

Interestingly, the SER and CAS configurations are identical except for the position of the feed. This single factor, however, results in large differences in membrane performance. In the series configuration,



(a) Two stage cascade with recycle compression (CASR)



(b) Two stage cascade with interstage compression (CAS)

RA-M-1732-19

Figure IV-5. Two stage cascade configurations for gas separations.

the feed and permeate streams are separated by only one stage, whereas two stages separate them in the cascade configuration. Thus, the cascade configuration provides a greater degree of separation but at the cost of a greater compression requirement.

Two Modules with Different Membranes

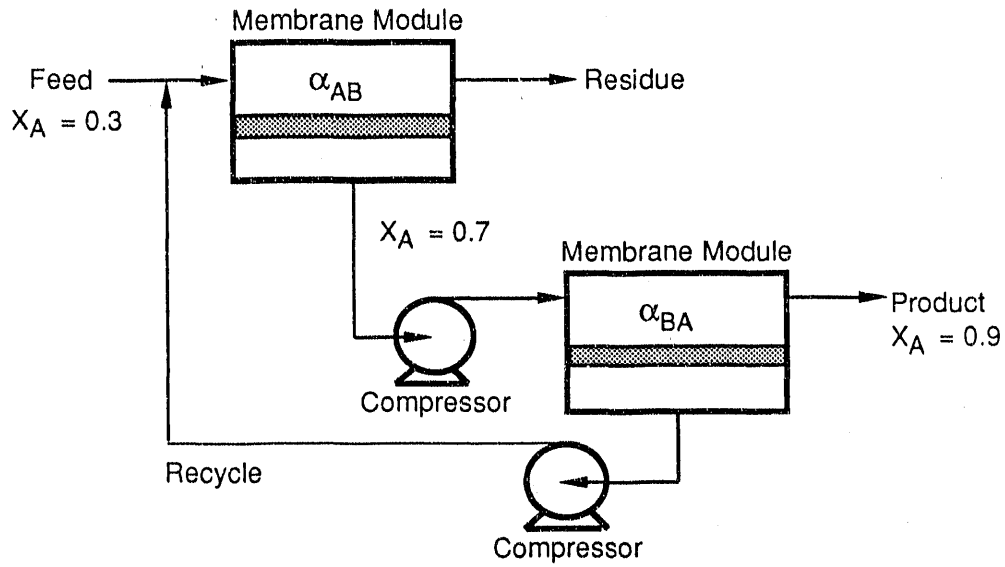
Using two modules also presents the option of using two different membrane materials. Often it is possible, by changing the manufacturing procedure, to modify a given membrane to increase its selectivity at the expense of lowering its permeability, or vice versa. It might be advantageous to use membranes modified in this way in a two module configuration. One module could contain a high selectivity/low permeability membrane and the other a low selectivity/high permeability membrane. The question arises as to which membrane should be used in each module. If a series configuration is under consideration, the highly selective membrane might be used in the first module to produce the most highly concentrated permeate, while the high permeability membrane would be used in the second stage to recover as much of the product as possible without using too large a membrane area.

If we are considering a cascade configuration, however, we might use the low selectivity/high permeability membrane first. In a two stage configuration the first stage always has the higher feed flow; therefore, it usually has the largest membrane area, and greater reductions in membrane area can be obtained by using the high permeability membrane in this stage. In the second stage, gas flows are smaller, and the greater membrane area required by the more selective but less permeable membrane may be acceptable. As well, when one membrane has a higher selectivity than another, a smaller pressure ratio would likely be used with the more selective membrane. This means increased compressor requirements in the stage containing the more selective membrane, which is another reason to put the high selectivity membrane in the second stage where the gas flow rates, and therefore the compressor requirements, are less.

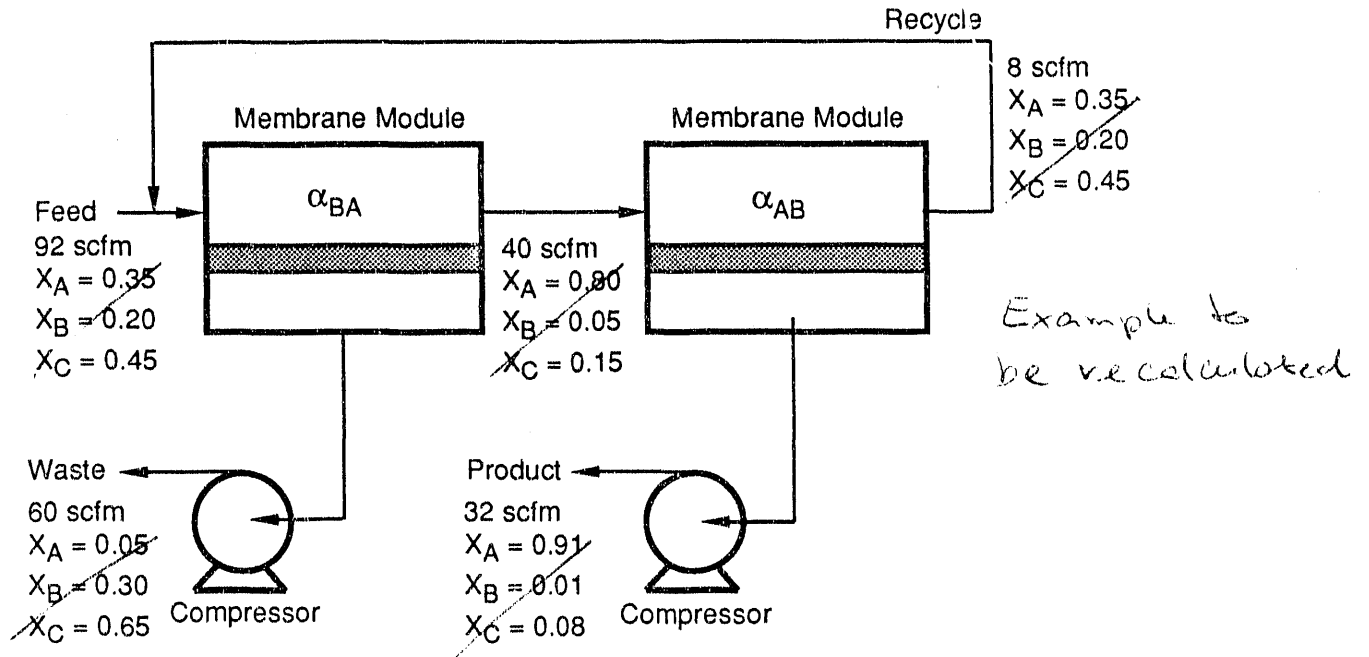
An interesting possibility is to use two membranes that differ not only in the degree of their selectivities and permeabilities but whose selectivities are the inverse of each other. That is, one membrane may be selective for component A over component B, while the second membrane is selective for B over A. Again, the question arises as to which membrane should be used in each module. In general, it is desirable to concentrate the minor component of the feed in the permeate stream. In this way, only a minor fraction of the feed must permeate the membrane, resulting in lower membrane area and compressor requirements than if the major fraction of the feed must permeate the membrane.

In general, the membrane material used in each module should be the material selective for the minor component in the feed to that module. Using this guideline, we can predict what configurations, and what specific applications, would benefit from using inversely selective membranes. In a two component system with a series configuration, the minor component is often the same in both modules, and inversely selective membranes would not be used. A cascade configuration, however, is likely to have different minor components in the feeds to the two modules, and the use of inversely selective membranes may be beneficial. A flow diagram illustrating the two component cascade system is shown in Figure IV-6.

When the system contains three components, with component C being the least permeable to both membranes, a series configuration might utilize inversely selective membranes to produce a waste stream, a recycle stream, and a product stream, as illustrated in Figure IV-6. With the cascade configuration and three components, some applications will benefit from inversely selective membranes and others will not, depending on the feed composition and membrane selectivities. As the number of components increases, predicting whether a certain application will benefit from inversely selective membranes becomes more difficult without performing detailed membrane performance calculations.



(a) Cascade configuration with two components.



(b) Series configuration with three components.

RA-M-1732-20

Figure IV-6. Separation systems which benefit from inversely selective membranes.

V MEMBRANE SYSTEM EXAMPLES

To demonstrate the performance characteristics of different configurations, performance calculations have been done for several configurations discussed in the previous section. As mentioned earlier, the pressure ratio is a variable whose value is specified by the process designer. Within the constraints on the value of the pressure ratio, the designer must determine the optimum pressure ratio that results in the lowest overall cost to perform the desired separation.

For each process considered in this chapter, the optimum pressure ratio was determined and the processing cost at this pressure ratio was calculated. The processing cost (PC) is the value that must be recovered per unit of product to pay for capital and operating expenses of the separation system and give a 15% return on capital investment. The separation systems evaluated in this chapter consists of membrane modules and compressors. Membrane costs were assigned an installed cost of \$24/ft² and a replacement cost of \$10/ft². A membrane lifetime of 5 years was used. Compressor expenses were calculated using the following formulas:

$$E_c = 4.36 \times 10^{-3} \cdot \left(\frac{k}{k-1}\right) \cdot N_s \cdot Q \cdot P_o \cdot \left[(CR)^{\frac{k-1}{k \cdot N_s}} - 1 \right] \cdot \frac{1}{f_c f_m} \quad (30)$$

where the number of stages, N_s , depends on the compression ratio, CR. In our calculations we used:

$$\begin{array}{ll} 27 > CR \geq 9 & N_s = 3 \\ 9 > CR \geq 3 & N_s = 2 \\ 3 > CR \geq 1 & N_s = 1 \end{array}$$

$$C = N_p \cdot I_f \cdot 1.045 \cdot \left(10^{(0.9583 \cdot \log(E_c/N_p) - 0.4114)} \right) \quad (31)$$

where

- C = installed cost (\$1,000s)
- CR = compression ratio (P_2/P_1)
- E_c = compressor power required (H_p)
- f_c = compressor efficiency
- f_m = motor efficiency
- I_f = installation factor
- k = ratio of specific heats ($= C_p/C_v$)
- N_p = number of individual compressors used in parallel
 - integer portion of $\left(\frac{EC}{S_{\max}} + 1 \right)$
- N_s = number of stages
- P_1 = suction pressure (psia)
- P_2 = discharge pressure (psia)
- Q = feed rate (CFM at intake conditions)
- S_{\max} = maximum compressor size (hp)

The compressor and motor efficiencies, f_c and f_m , have values of 0.85 and 0.90, respectively. I_f has a value of 3, k has a value of 1.4 and S_{\max} equals 4,000 hp. We have assumed a labor requirement of 0.03 men/shift.

The capital and operating costs are included in a discounted cash flow program that results in the processing cost (expressed as dollars per unit of product).

Example Application

The application for which the configuration comparisons are given is the separation of a mixture of two components, H_2 and N_2 , where H_2 is the product to be concentrated in the permeate stream. The feed conditions and membrane properties are given in Table V-1. The feed conditions are similar to those obtained in an air-blown coal gasification process after

Table V-1

FEED CONDITIONS AND MEMBRANE PROPERTIES FOR EXAMPLE APPLICATION

Feed Conditions:

mole fraction of H ₂ (X _{FH})	-	0.34
mole fraction of N ₂ (X _{FN})	-	0.66
temperature (°C)	-	150
pressure (psia)	-	300
flow rate (scfm)	-	10,000

PEI Membrane Properties:

PNF* of H ₂	-	6.7 x 10 ⁻⁴	$\frac{\text{cm}^3(\text{STP})}{\text{cm}^2\text{-s-cm Hg}}$
PNF* of N ₂	-	9.9 x 10 ⁻⁶	$\frac{\text{cm}^3(\text{STP})}{\text{cm}^2\text{-S-cm Hg}}$

*PNF = Pressure normalized flux (permeability/membrane thickness).

CO to H₂ shift and acid gas removal. (The conditions in the real process would be slightly different due to the presence of impurities such as H₂S, CO, and CO₂.) The membrane properties are those of the poly-[etherimide], PEI, membrane developed by MTR for this project. We will assume that the use of vacuum pumps is to be avoided; thus, the permeate pressure can never be less than atmospheric. Since the feed pressure is 300 psia, the minimum allowed value for the pressure ratio is 0.05.

To compare the different configurations, we established two criteria for the product stream: in all cases, 95% of the H₂ contained in the feed stream must be recovered in the permeate stream; and the product purity must be the same for all processes to be compared. Since we do not expect the same configuration to be best for all product purities, the performance calculations will be made over a range of product purities from 80% H₂ to 99.8% H₂.

Six configurations will be examined: single module (SM, Figure IV-3a); single module with recycle (SMR, Figure IV-3b); series (SER, Figure IV-4); and cascade with interstage compression (CAS, Figure IV-5b). The two remaining configurations use a different membrane in each stage of a CAS configuration. In one case, CAS-SP, the first stage will contain a high selectivity/low permeability membrane and the second stage will contain a low selectivity/high permeability membrane. The second case, CAS-PS, uses the two membranes in the opposite order of CAS-SP. The properties of the high permeability membrane are the same as those listed in Table V-1. Hypothetical properties of a high selectivity membrane are:

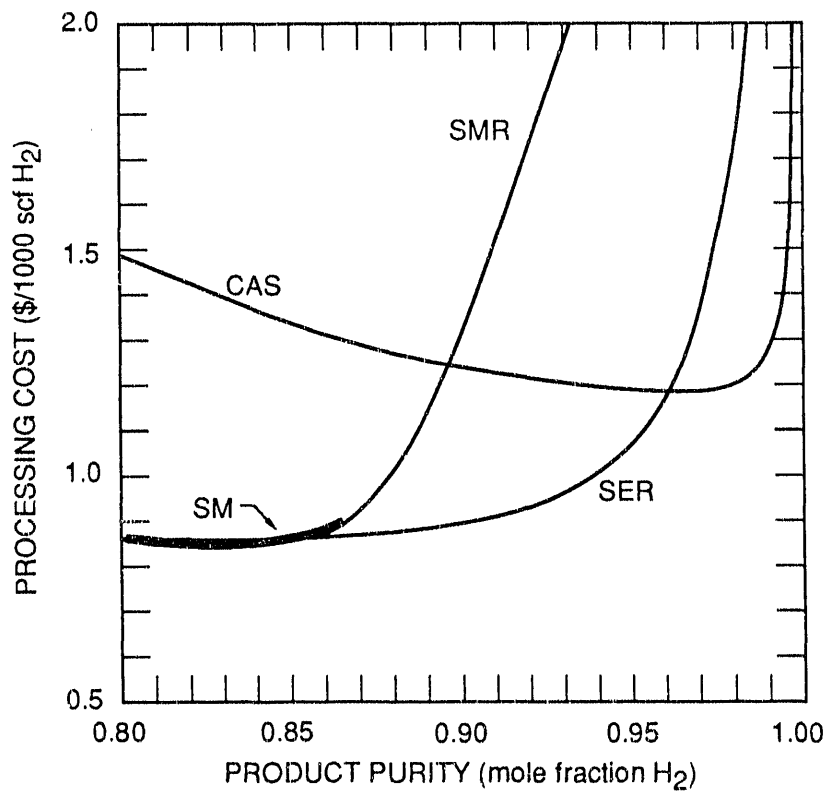
$$\text{PNF of H}_2 = 1 \times 10^{-4} \frac{\text{cm}^3(\text{STP})}{\text{cm}^2 \cdot \text{s} \cdot \text{cm Hg}}$$

$$\text{PNF of N}_2 = 1 \times 10^{-6} \frac{\text{cm}^3(\text{STP})}{\text{cm}^2 \cdot \text{s} \cdot \text{cm Hg}}$$

The performance of these two configurations will only be examined at product purities of 0.96 and 0.98, again requiring 95% recovery of H₂.

Performance Calculation Results

The processing cost for configurations SM, SMR, SER, and CAS are shown in Figure V-1. With the SM configuration, the maximum obtainable permeate purity while still recovering 95% of the H₂ is 86.2% H₂. To obtain higher purities, one of the other configurations must be used. For low product purities (less than ~ 86% H₂), the processing costs for configurations SM, SMR, and SER are the same. Upon examination of the optimized process conditions at these low product purities, we find the recycle rate was zero in SMR, and the second stage membrane area was reduced to essentially zero for SER; thus, the optimum SMR and SER configurations reduce to SM when the product purity is less than 86%. Moreover, the optimum SMR configuration reduces to SM whenever the desired product purity can be obtained with SM. In the case of SER,



RA-M-1732-21

Figure V-1. Processing cost as a function of product purity.
 In all cases 95% of H₂ is recovered.

however, in a small range of product purities the optimum SER configuration does not quite reduce to SM, even though the desired purity can be obtained with SM. This range is small (85.6% A to 86.2% A), and in general if the SM configuration can produce a product of the desired purity, this configuration is better than either SMR or SER.

CAS does not also reduce to SM at low purities because two stages separate the product from the feed streams. In the other configurations, the product and feed streams are separated by only one stage, and all can be reduced to the SM configuration by setting the flow rates of certain streams to zero. For purities above those obtainable with SM, SER always has a lower processing cost than does SMR. The processing cost with SER begins to increase sharply near a product purity of 96%, and beyond this purity CAS has the lowest processing cost of all configurations.

In Figure V-1, a shallow minimum occurs in the processing cost curves for both SM (which includes the optimized SMR and SER configurations) and CAS. For product purities lower than the value corresponding to the minimum, the processing cost increases with decreasing product purity. This behavior is unexpected; in most separation processes, a decrease in product purity corresponds to a decrease in processing cost. This behavior is the result of the different process conditions that apply when producing different purity permeates. To lower the product purity in this example, the pressure ratio (the only variable which is not fixed) must be increased. The increased pressure ratio reduces the driving force for mass transfer across the membrane, and the membrane area must be increased to maintain 95% recovery of H_2 . Although the larger pressure ratio reduces the compression costs, these savings are more than offset by the increased membrane expenses, and the net result is increased processing cost. The product purity value at which this minimum occurs is determined by the process and economic conditions of each application.

If a membrane system could produce a product with a higher purity than necessary and at less cost than it could produce the desired, lower purity product, it would be sensible to produce the high purity product

and dilute it with untreated feed to the desired purity. This flow scheme, shown in Figure V-2, in which only part of the feed is treated by the membrane system and then is mixed with the remaining untreated feed will be called partial feed bypass (PFB).

The product purity that can be produced with PFB can be determined using the conservation of mass equations,

$$F_o + F_m = F_r \quad (32)$$

$$X_F F_o + Y_p F_m = Z_p F_T \quad (33)$$

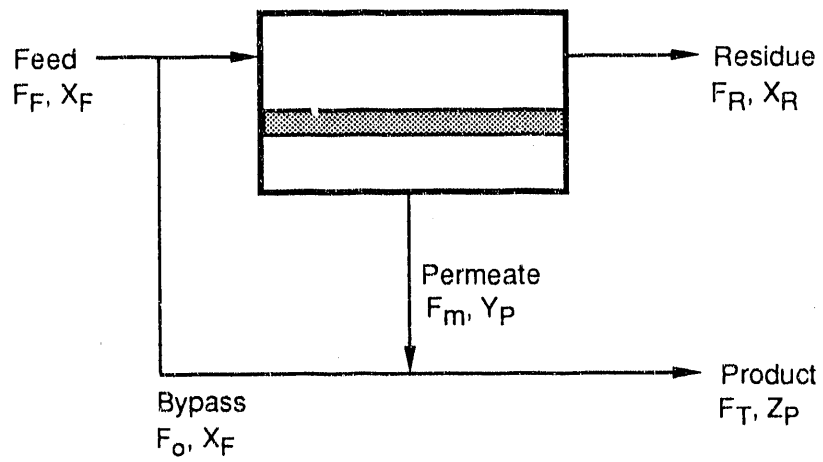
where F_o , F_m , and F_T are the flow rates of the bypass, permeate, and product streams and X_F , Y_p , and Z_p are the mole fractions of H_2 in the bypass, permeate, and product streams respectively. Since the total cost for processing the product stream is equal to the sum of the costs for processing the bypass and permeate streams, the following equation can be written:

$$(X_F F_o) PC_o + (Y_p F_m) PC_m = (Z_p F_T) PC \quad (34)$$

In this equation, PC_o is the processing cost of the bypass stream (equal to zero in this example), PC_m is the processing cost of the permeate stream, and PC is the processing cost of the product stream. (The mole fractions are included in the above expression because the PCs are based on quantities of pure H_2 .)

Using the three above equations, an expression can be derived for PC :

$$PC = X_F / Z_p \left(\frac{Z_p - X_F}{Y_p - X_F} \right) PC_o + Y_p / Z_p \left(\frac{Z_p - X_F}{Y_p - X_F} \right) PC_m \quad (35)$$



RA-M-1732-22

Figure V-2. Partial feed bypass scheme.

Only a portion of the feed must be processed by the membrane system.

When PC_0 equals zero, this expression reduces to

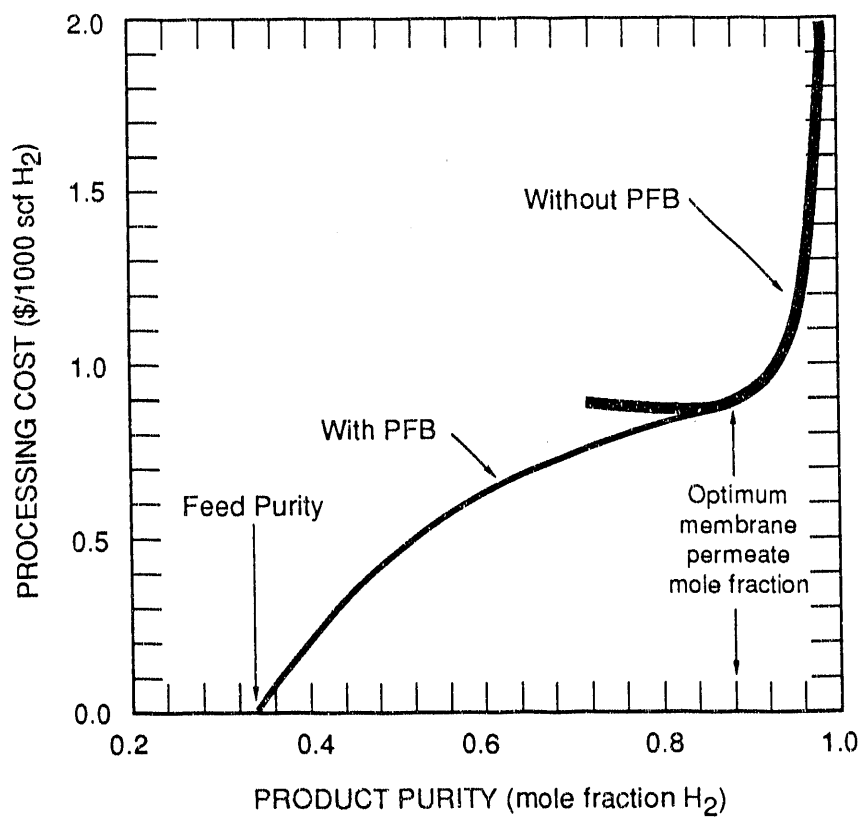
$$PC = Y_p/Z_p \left(\frac{Z_p - X_F}{Y_p - X_F} \right) PC_m \quad (36)$$

The value for Y_p (with corresponding PC_m) is a design variable and must be chosen to give the lowest value for PC. Possible Y_p values can be taken from curves such as those in Figure V-1 until the optimal value is found. Figure V-3 shows the optimum PFB curve with Y_p equal to approximately 0.88. If a higher purity product were desired, PFB would not be used.

Figure V-4 shows the processing costs with PFB for the four configurations included in Figure V-1. The dashed lines represent the region where PFB would be used. The solid lines represent the cases in which PFB should not be used; all the feed should be treated by the membrane system. Figure V-4 shows that when PFB is included in this example, SER results in the lowest processing cost for product purities less than approximately 0.96. Above 0.96, CAS is the configuration with the lowest processing cost.

In our calculations, we specified that 95% of the H_2 entering the membrane system must be recovered. With PFB however, because a portion of the feed does not go through the membrane system, the overall H_2 recovery is slightly higher. The increased number of calculations necessary to calculate the PFB processing cost with an overall recovery of exactly 95.0% requires more effort than is justified for this example. (The H_2 recovery with PFB using the cascade configuration to make a 90% H_2 product stream is 95.2%).

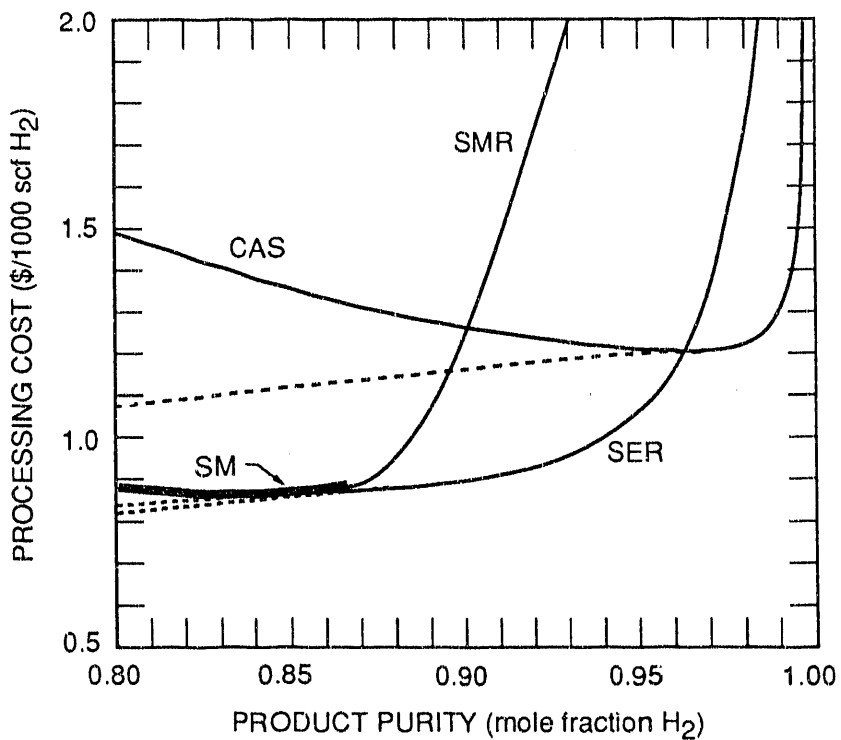
These processing costs curves are valid for this example only. Under different conditions, both the processing cost curves and the region where PFB should be used would change. For example, if the membrane system fractional recovery was lowered from 95% to 90%, we would expect all processing costs to be reduced, the point where the SER and



RA-M-1732-23

Figure V-3. Processing cost with and without PFB.

In this example the optimum permeate mole fraction is approximately 0.88.



RA-M-1732-24

Figure V-4. Processing costs for the four different configurations with PFB.

The dashed lines represent the costs when PFB is used.

CAS curves intersect would change, and the point where use of PFB begins would move to the left. Similarly, the feed composition, membrane properties, and economic parameters all affect the processing cost curves.

Two additional configurations, CAS-SP and CAS-PS (cascade configurations that use a different membrane material in each stage), were evaluated. The parameters other than the membrane properties are the same as in the previous example except PFB was not included and only two product compositions were examined. The processing costs resulting from these two configurations are given in Table V-2 along with the values from the four previously discussed configurations. From the discussion in the previous section, we expect that placing the high selectivity membrane in the second stage will result in a lower processing cost than placing it in the first stage; the results confirm this expectation. For configuration CAS-PS, the PC to produce 98% H₂ is less than to produce 96% H₂. Thus, CAS-PS (and probably CAS-SP) should also benefit from PFB.

Table V-2

PROCESSING COSTS FOR SIX DIFFERENT
MEMBRANE SYSTEM CONFIGURATIONS
(PFB not included)

<u>Configuration</u>	<u>PC (\$/1000 scf H₂)</u>	
	<u>Product</u>	<u>Purity</u>
	<u>0.96</u>	<u>0.98</u>
SM	--	--
SMR	3.90	8.57
SER	1.19	1.73
CAS	1.20	1.22
CAS-SP	2.16	2.18
CAS-PS	1.75	1.54

The processing costs for both these configurations are greater than for CAS (which uses the high permeability/low selectivity membrane in both stages). Thus, in this example the penalty for reducing the permeability in one stage (by a factor of 9.9) is not compensated for by increased selectivity (from 68 to 100). Considering that the smallest value for the pressure ratio, γ , allowed in this example is 0.05, we would not expect that modifying the membrane to increase the selectivity (which is already much larger than $1/\gamma$) would result in a significant improvement in membrane performance. However, the decrease in permeability (that accompanies the increased selectivity) would significantly increase membrane costs, and it is not surprising that in this example the processing cost is increased by using the modified membrane in one stage. If, however, the modified membrane had had a lower selectivity and higher permeability (instead of vice versa), using the modified membrane in one stage probably would have lowered processing costs.

In this section we have discussed methods for determining when one configuration is better than another for a given application. In general, CAS is better economically than SER or the single stage configurations for obtaining higher purity products, and SER is best for lower purity products. Because of its simplicity, SM may replace SER when low product purities are required, even though the predicted costs are slightly lower with SER; single stage with recycle, however, is never the best configuration. When two different membranes are used in each stage of a two stage configuration, the application conditions and membrane properties will determine whether using one of each membrane type results in lower processing cost than using the same membrane type in both stages.

VI CONCLUSIONS

We draw two main conclusions from this study: the first concerns the adequacy of computer models to predict membrane performance, and the second concerns the membrane system configuration best suited to a particular set of operating conditions. The model resulted in predictions that agreed well with experimental results using different feed flow rates and compositions provided that at least one mixed-gas experiment was performed from which gas permeabilities could be calculated. However, the model did not result in agreement between predicted and experimental results for the separation of gas mixtures if the gas permeabilities used were obtained in pure gas experiments. We believe this disagreement is primarily due to plasticization of the membrane by CO_2 , an effect that is a function of the partial pressure of CO_2 .

Our comparison of several membrane configurations showed SM to be most economical for low product purities, SER for medium product purities, and CAS for high product purities. If a partial feed bypass arrangement is used, however, SER is most economical for low and medium product purities, while CAS is still most economical for high product purities.

REFERENCES

- Chern, R. T., W. J. Koros, E. S. Sanders, S. H. Chen, and H. B. Hopfenberg, In: T. E. Whyte Jr., C. M. Won, and E. H. Wagener (Eds.), *Industrial Gas Separation*, ACS Symposium Series No. 223, American Chemical Society, Washington, DC, 1983.
- Matson, S. L., J. Lopez, and J. A. Quinn, "Separation of Gases With Synthetic Membranes," Chem. Eng. Sci., 38, 4, pp. 503-524, 1983.
- Pan, C. Y., "Gas Separation by High Flux, Asymmetric Hollow Fiber Membrane," AIChEJ, 32, pp. 2020-7, 1986.
- Pan, C. Y., and H. W. Habgood, "An Analysis of the Single-Stage Gaseous Permeation Process," Ind. Eng. Chem., Fundam., 13, 4, pp. 323-331, 1974.
- Peinemann, K., J. M. Mohr, and R. W. Baker, "The Separation of Organic Vapors from Air," AIChE Symp. Series, No. 250, 82, pp. 19-26, 1986.
- Shampine, L. F., H. A. Watts, and S. Davenport, "Solving Non-Stiff Ordinary Differential Equations - The State of the Art," Sandia Laboratories Report SAND75-0182, 1975.
- Shindo, Y., T. Habuta, H. Yoshitome, and F. Inoue, "Calculation Methods for Multicomponent Gas Separation by Permeation," Sep. Sci. and Tech., 20, 5 & 6, pp. 445-459, 1985.

END

**DATE
FILMED**

8 / 27 / 92